Ocean Engineering 188 (2019) 106268

Contents lists available at ScienceDirect

Ocean Engineering

journal homepage: www.elsevier.com/locate/oceaneng

Impact of simulation model fidelity and simulation method on ship operational performance evaluation in sea passage scenarios

Jørgen Bremnes Nielsen [a,*], Endre Sandvik [a], Eilif Pedersen [a], Bjørn Egil Asbjørnslett [a], Kjetil Fagerholt [b]

[a] Department of Marine Technology, The Norwegian University of Science and Technology, Trondheim, Norway
[b] Department of Industrial Economics and Technology Management, The Norwegian University of Science and Technology, Trondheim, Norway

ABSTRACT

In this paper, we present and investigate important factors that influence a vessels fuel consumption during operation and what model fidelity that is required to adequately capture these factors in fuel consumption estimations. Our study focuses on evaluating effect of model fidelity and the methodology used to assess the ship behaviour in operational conditions. Operational performance is affecting cost of operation and estimations of operational performance is used in design development, operational research and as basis for emission analysis, affecting decision making at an operational and technical level. A comprehensive case study is presented where we compare fuel consumption and engine operational profile for time domain and discrete-event simulations, and a static statistical model. Of the factors that have been included in the study, variation in propeller loading and consequently propulsion efficiency is the most prominent physical factor for estimation of required power and fuel consumption. Further, the ability to replicate realistic scenarios using simulators has a significant effect on our understanding of how operational and environmental factors affect operational performance.

1. Introduction

Shipping, although being an energy efficient mode of transport, is a significant contributor to global emissions such as green house gases (GHG), NO_x, SO_x and PM (Buhaug et al., 2009; Corbett et al., 2007a; Eyring et al., 2005; Klimont et al., 2017), which are affecting global climate, human health and the environment (Eyring et al., 2010; Corbett et al., 2007b; Kampa and Castanas, 2008). The International Maritime Organization (IMO) is addressing the negative impact of shipping on global climate, human health and the environment by issuing regulations, requiring emission reduction such as the NO_x emission limits of MARPOL Annex IV and the Energy Efficiency Design Index (EEDI). Several new technologies are being evaluated for use in marine power systems aiming at increasing transport energy efficiency (Bouman et al., 2017) and reducing emissions (Fujibayashi et al., 2013; Hiraoka, 2016; Gregory and Confuorto, 2012; Di Natale and Carotenuto, 2015). Evaluating a large number of potential technical solutions require cost effective evaluation methods. In addition these methods have to capture the nature of ship operation to provide valuable information on novel system solution performance.

There are currently promising methods being put forward using data-driven statistical methods for increasing the ability to predict the operational performance of a ship (Yoo and Kim, 2019). While data-driven methods are useful for generating operational performance models of already existing ships, the ability to predict effects of changes in a system design is limited as there exists no measurement data for non existing systems. Improving system solutions depends on an ability to evaluate the effect of design changes of which there are currently limited performance information. This is commonly achieved by using mathematical modelling and numerical simulation to predict the behaviour and performance. While modelling and simulation is a powerful method, enabling the use of computers to predict behaviour and performance of physical artifacts, there are still limitations. Commonly, model development requires making simplifications which can affect the validity of the simulation results. In the evaluation of novel systems and in design optimization it is common to simplify the effect of the operational conditions and operational decisions, such as single load point evaluation (Song and wei Gu, 2015; Larsen et al., 2014) and simplified operational profiles (Gully et al., 2009). The possibility of using data from these simplified analyses to predict a systems performance in operational conditions is limited as the cases used are remote from operational conditions. Increasing our understanding of the potential of novel systems requires evaluation in an operational context to ensure that solutions do perform according to expectations in realistic operating conditions, and not only in theoretical cases (Lindstad and Bø, 2018).

Evaluating a system's operational performance in a seaway is a challenging undertaking. This is due to the large number of different domains involved, the need for large amounts of information, and the

* Corresponding author.
E-mail address: jorgen.b.nielsen@ntnu.no (J.B. Nielsen).
URL: https://www.ntnu.no/ansatte/jorgen.b.nielsen (J.B. Nielsen).

https://doi.org/10.1016/j.oceaneng.2019.106268
Received 19 March 2019; Received in revised form 1 July 2019; Accepted 4 August 2019
Available online 26 August 2019

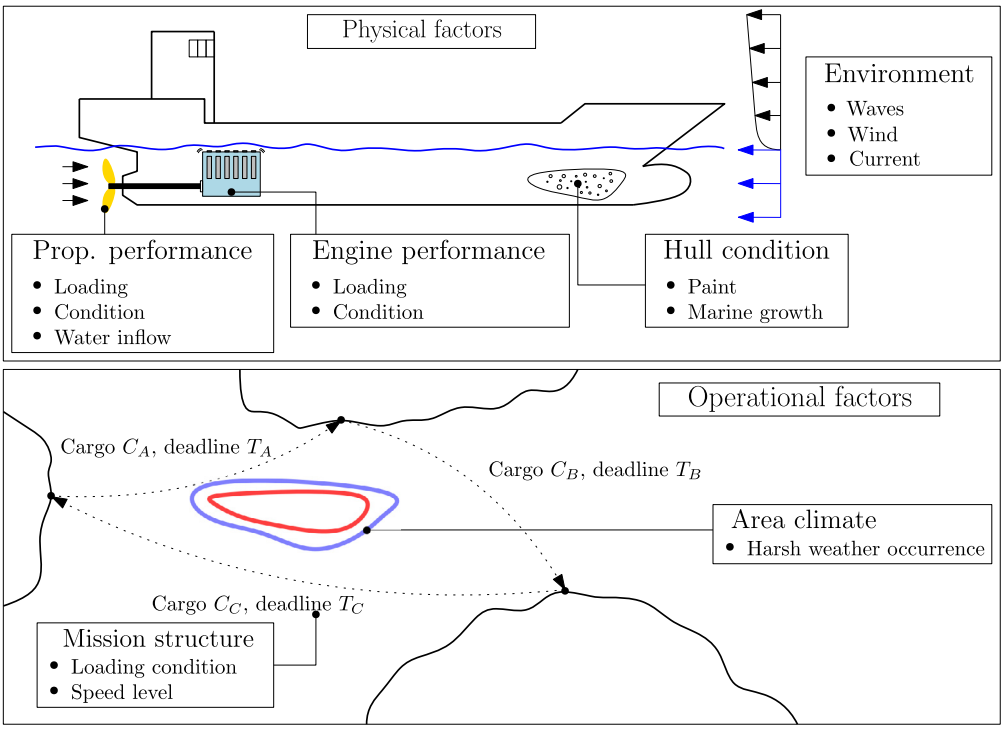

Fig. 1. Major physical and operational fuel consumption factors.

difficulty of capturing the physical phenomena sufficiently accurate in a mathematical form that can be calculated within a reasonable time frame. Seaway performance evaluation depends on describing the operation conditions consisting of waves, current and wind, the hull and propeller performance in the current sea states and power production with dynamic loads. In addition, a ship is free to change course, making the encountered weather a function of operational choices made at different levels in the organization operating the ship.

Establishing these relationships involves abstraction of relevant phenomena into mathematical models that can be used to predict the performances through either analysis or simulation. There are trade-offs between model fidelity, model development cost, required calculation or simulation effort and prediction validity of the model that have to be considered when developing models for operational performance evaluations. Estimating power demand, transmission efficiency and power production efficiency using models of appropriate fidelity balances the need to capture the effect of design variations and the ability to evaluate a high number of design concepts. Several approaches for modelling operation performance have been used in the literature. Corbett et al. (2009) used still water and a cubic relationship between speed and fuel consumption with constant specific fuel consumption to evaluate the effect of speed reduction on emissions of CO_2 on a fleet level. For the same purpose of evaluating effect of speed reduction on CO_2 emissions on a fleet level, Lindstad et al. (2011) expanded the still water assumption to include added resistance due to waves when calculating the power demand. In addition propeller efficiency as function of vessel speed was included to account for transmission efficiency. However, added resistance is based on an estimated average significant wave height of 2.5 metres and a fixed specific fuel consumption. In the evaluation of different power system setups, fuels and hull designs, Lindstad and Bø (2018) further expanded the power production efficiency model to include specific fuel consumption as function of engine power. Significant wave height was also expanded to a set of expected significant wave heights with fractions of sailing time spent in the different wave conditions. In the work on an operational performance prediction model, Lu et al. (2015) used sea trail data to establish the relationship between the power demand and engine power and the test bench specific fuel consumption curve to establish fuel consumption. In the work of Prpić-Oršić and Faltinsen (2012) estimated the effect of speed loss in a sea way due to added resistance and the effect of wave on the propeller performance. However, the fuel consumption was based on a constant power assumption with a fixed fuel consumption per day. In Tillig et al. (2017) engine fuel consumption is based on model taking into account the working point of the engine (power and rpm), with torque limits and rpm limits. While different modelling assumptions are used, it is difficult based on the available literature to evaluate the importance of the different assumption and whether including additional factors are worth the effort.

In the present paper, we evaluate the effect of model fidelity considering alternative modelling approaches for capturing factors affecting ship operational performance. Three fundamental aspects are included in the evaluation; power demand, power transmission efficiency and power production efficiency. Two models with different fidelity and two simulation methods are compared, where a high fidelity time domain model is used for reference. The novelty of the paper is the comparison of state of the art models for power demand, transmission efficiency and power production efficiency used in operational analysis of effect of system design and operational policies with a state of the art time domain simulation model of the same system. The differences will be quantified in a case study where three different operation policies are simulated for 12 voyages equally spaced over one year.

This paper is organized into six sections. The next section addresses the identification of factors relevant for estimating operational performance focusing on fuel consumption. Section 3 presents the case study and the different models that are to be compared. Section 4 presents the results focusing on the effect of different factors and the effect of model fidelity. Section 5 discusses the results in the context of trade-offs between prediction validity versus the cost of modelling and simulation and the availability of the different models for representing novel designs. Finally, the work is concluded in Section 6.

2. Estimating fuel consumption in operational conditions

Fuel consumption is considered to be a variable of special interest. From a societal and economic perspective, it represents a measure of emission level and costs. From a modelling perspective, it requires modelling of processes and factors spanning from organizational policies to engine performance at sea. This section presents our approach towards modelling ships in operational conditions and estimating fuel consumption. First, it considers the physical and operational factors which is present in a maritime transportation operation. The occurrence and interaction between these factors are discussed and then categorized according to how they affect the fuel consumption. Three categories are used; power demand, power transmission efficiency and power generation efficiency, which are needed to calculate the fuel consumption. Further the implementation of the different factors into simulation models are illustrated. Finally, the system is presented in a generic form consisting of the transformation of fuel to transport work and categorization of fuel consumption factors.

2.1. Fuel consumption factors and domains

In the present work, the term "operational conditions" refers to the physical environment the ship operates in, i.e. the wave, current and wind conditions encountered by the ship. Fig. 1 shows the major factors for fuel consumption in operational conditions. Physical factors determine the fuel needed to overcome resistance within a given environmental condition at a given speed. They arise from hydrodynamic and mechanical engineering domains and are associated with the technical description of the ship. Operational factors are linked to the overall objective for the ship to be present at its location carrying a given cargo load. These factors arise from human decision making and operational policies impacting the choices made by the ship owner and ship master, processes most commonly addressed in operations research. Maritime transportation is commonly divided into liner, industrial and tramp shipping, giving rise to varying requirements in term of speed management and schedule. Meeting these requirements entails choices affect the vessel's behaviour through operational and tactical decisions. The different factors are not independent or static and are determined by design, the interaction within and between operational and physical factors, and the changing condition of the system with time and use.

2.2. Factor interaction

Fig. 2 shows our model for factor interaction. On top, we have the operation, i.e. the context for applying the vessel to do a specific mission within a given set of constraints. In the area of operation, weather conditions are present which affects the power demand through resistance. The knowledge of this effect creates a feedback-loop in the form of operational reevaluation, from which the operation and sea passage behaviour may be altered. The interaction between operational considerations and occurring environmental conditions results in a set of sea states and vessel speeds for the operation. Combining sea state and operation allow us to express vessel resistance and required propulsion power, giving us the basis for the operation power demand. Further, propeller thrust is generated at a corresponding efficiency level depending on the propeller loading and interaction from waves and current. Hence, our modelling approach provides a link between operation and fuel consumption, spanning from high-level operational tasks and decisions to low-level physical effects and demand for the power plant.

2.3. Factor categorization

Fig. 3 shows the system boundaries with fuel and mission as input and transport work as output. Estimating the conversion of fuel to transport work through a mission depends on determining the power demand, the power transmission efficiency and the power generation efficiency. Environment is included as an input affecting the factors in the three categories and emissions are an unwanted bi-product of the process. For propulsion, power demand is associated with the ability to overcome resistance. Power production is the process of converting potential energy in the fuel to mechanical energy using a power plant operating in a given condition. Between power demand and power production is the transfer efficiency process, transporting energy from the power plant to the propeller, generating thrust and performing transportation work. The generic layout of Fig. 3 is applicable for modelling fuel and energy requirements for all types of ship types and propulsion systems. It also serves as a means in the present paper for communicating and discussing the implications and effects of modelling assumptions on fuel consumption estimates.

3. Case study

A comprehensive case study has been conducted to test the impact of the modelling choices and simulation method in operational performance prediction. Performance evaluation is selected to be carried out by replicating a crossing of the North Pacific ocean from Tokyo to San Francisco. This area was chosen to ensure a sufficient simulation length which facilitate the occurrence of multiple weather systems along the route. KVLCC2 (Kim et al., 2001) was chosen as the case vessel as it is an academic hull where data is readily available. The engine modelled is a Wartsila 8RT-FLEX68D rated to 25,040 kW at 95 RPM. The vessel is equipped with a fixed pitch propeller where the design has been adapted to the engine and the hull.

3.1. Model descriptions

As discussed in Section 2 there are several factors that affects the power demand, the power production and the power transmission. In this section, models used in the case study for capturing these factors are presented.

3.1.1. Model 1

Model 1 is based on a transient diesel engine model typically used to evaluate the effect of transient loads on engine performance (Rakopoulos and Giakoumis, 2006). Power demand is calculated by a vessel model and a propeller model. The propeller inflow is estimated by using ship stern motions ROAs. The RAOs are calculated using linear strip theory, utilizing potential theory and pressure integration using ShipX Veres developed by Sintef Ocean (previously MARINTEK). The propeller is represented by a one-quadrant model with thrust and torque coefficient curves estimated by using the open source Openprop software which is based on lattice lifting line theory. Javafoil (Hepperle, 2018) has been used to calculate frictional drag. Effect of ship motion and inflow on propeller torque and thrust has been included according to Taskar et al. (2016). The engine model is a dynamic model developed by Yum et al. (2017) capable of capturing interactions with the varying propeller load and predicting performance in dynamic loads. Introducing dynamic models significantly increases the information demand and the computational efforts required to estimate the performance. The vessel is modelled using a one-dimensional vessel model where only surge motion is considered. Added resistance has been calculated using strip theory, utilizing potential theory and pressure integration also by using ShipX Veres. Different significant wave heights (Hs), peak wave periods (Tp) and encounter heading combinations (α) has been used for calculating added resistance in irregular waves with the Pierson Moskowitz wave spectrum. Added resistance coefficients has

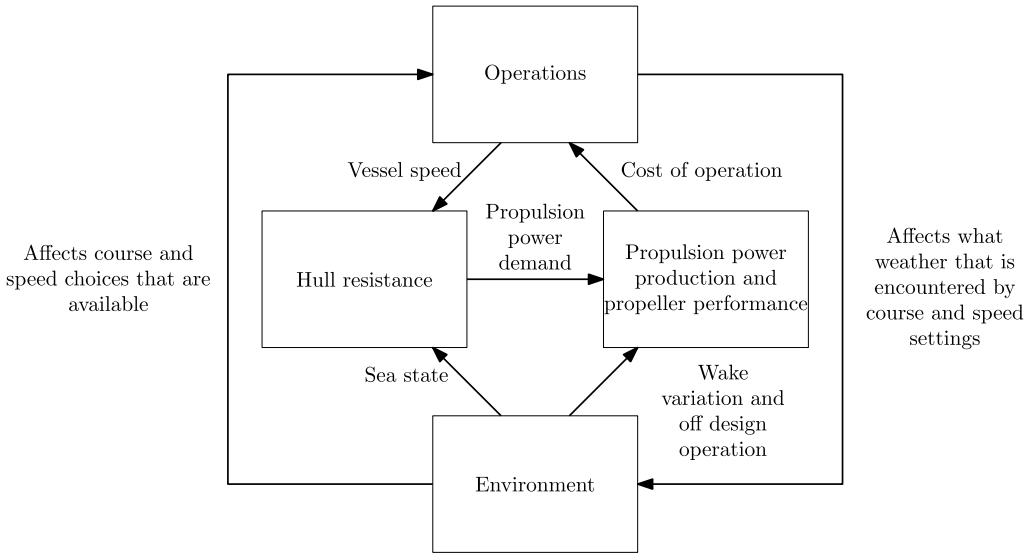

Fig. 2. Interaction between important aspects from a modelling perspective when recreating a real seaway operation.

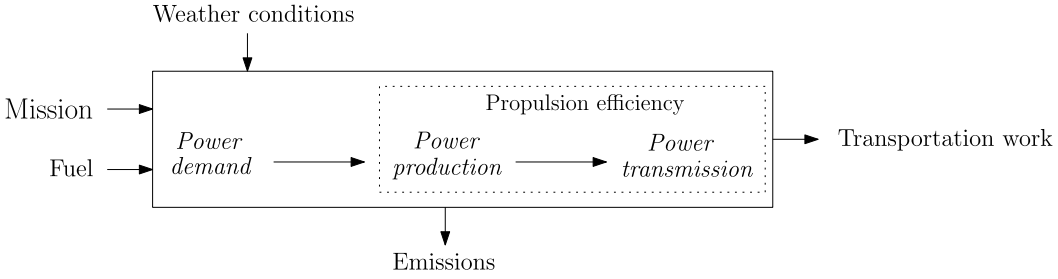

Fig. 3. Generic system model for ship fuel consumption analysis.

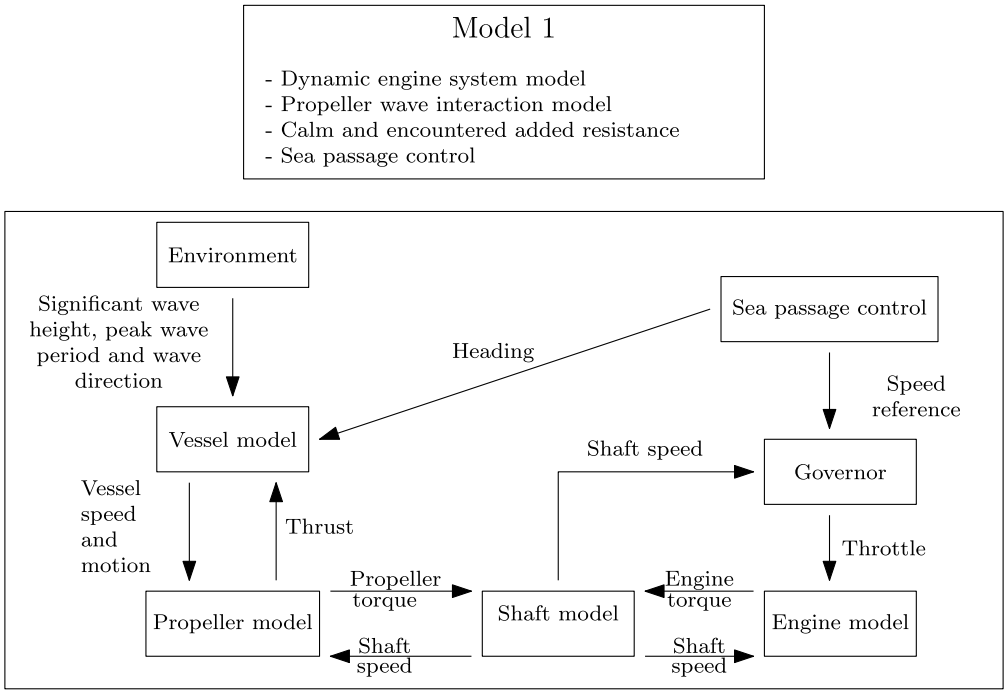

Fig. 4. Model 1 implementation.

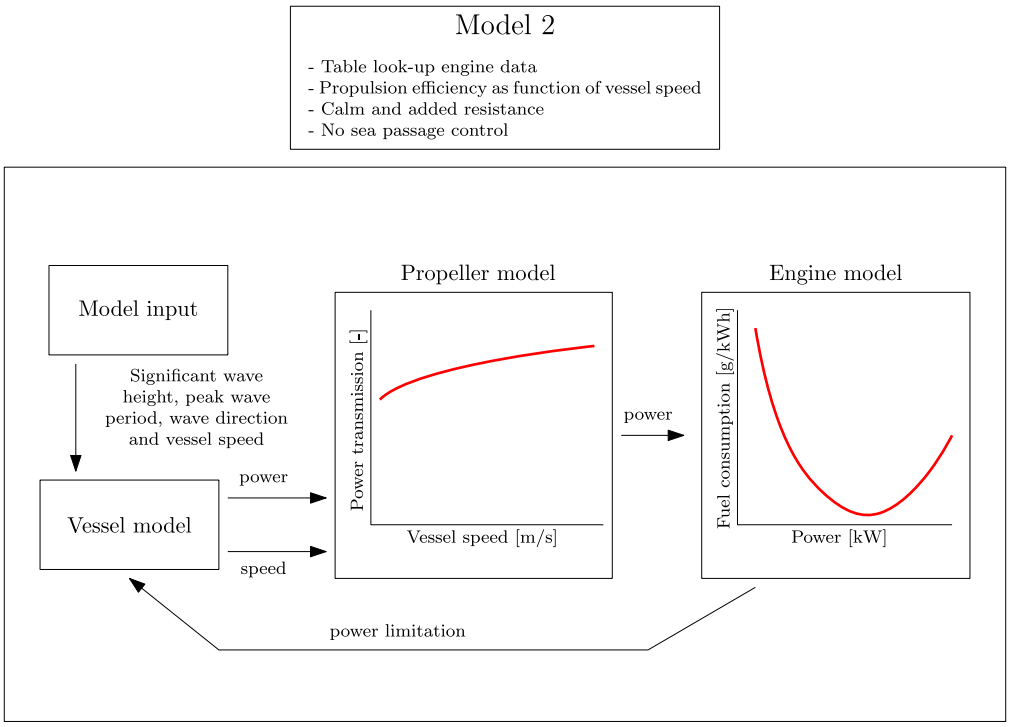

Fig. 5. Model 2 implementation.

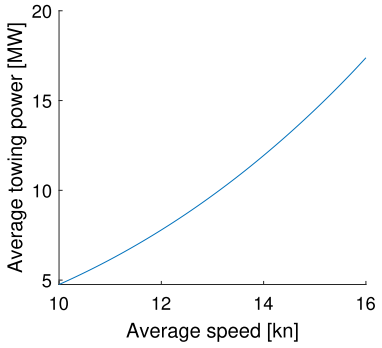

Fig. 6. Relationship between required average speed and engine power demand estimated based on the static statistical approach.

been calculated according to the method by Loukakis and Sclavounos (1978) using ShipX Veres. Fig. 4 shows the details of the model and the variables exchanged between the different sub models.

Model 1 is dependent on a sub-model for replicating a sea passage generating the sea state encountered based on position, time and prevailing weather. The simplest approach would be to select a great circle route, however such an approach to sea passage modelling would not take into account the freedom a ship and its captain have to select routes that avoid harsh weather etc. Sandvik et al. (2018) addresses the importance of active speed and course decision making for understanding the performance of ships during sea passage, and proposes a model for controlling sea passage behaviour in simulation models. The model adjusts vessel heading and speed as a function of two variables; target speed V_0 and schedule delay cost rate κ. The objective function minimizes voyage fuel consumption and delay costs taking into consideration weather within a 72 h horizon and estimated ship performance.

Wave conditions are based on hindcast data using the ECMWF ERA5 database (ECMWF ERA5, 2018). An assessment of three wave hindcasts including the ERA5 predecessor ERA-Interim has been carried out by Campos and Soares (2016) for the North Atlantic, which concluded that the data shows minor differences in non-extreme situations while there are significant differences in extreme situations. For the objective of this paper discrepancies in the extreme situations will have limited impact on the predictions as the time spent in extreme situations is very limited compared to the time spent in non-extreme situations. Campos and Soares also states that ERA-Interim is the preferred choice for non-extreme analysis. The impact of wind and current has not been considered in this case study.

3.1.2. Model 2

Model 2 is based on static performance estimation using still water engine performance curves and power transmission efficiency estimated as a function of vessel speed only, with a model suggested by Lindstad and Bø (2018):

$$\eta_D = \eta_d(j + k\sqrt{(v/v_d)}) \quad (1)$$

where η_D is the propulsion efficiency, η_d is the propulsion efficiency at design speed and v_d is the design speed. j and k are constants used to fit the efficiency, where $j + k = 1$. The fuel consumption is calculated based on the still water specific fuel consumption curve from Model 1. Propulsion efficiency η_D has been fitted to the propulsion efficiency of the Model 1 in still water conditions. Power demand is calculated with the same model as in Model 1 with both still water resistance and added resistance due to waves. Fig. 5 shows the details of the model and the variables exchanged between the different sub models.

Model 2 does not include any method for generating individual voyages. Therefore two approaches for estimating encountered sea states are used. In the first approach, voyage data from Model 1 is used to calculate still water and wave added resistance based on observed significant wave heights, wave periods, vessel speed and wave encounter angle. In the second approach, added resistance has been included by estimating expected sea states and power demands using a static statistical approach based on wave distribution parameters from DNVGL (2017) presented in table C-5. Fig. 6 presents the relationship between average speed and estimated average engine power demand, taking into account the effect of expected speed loss. This approach reduces

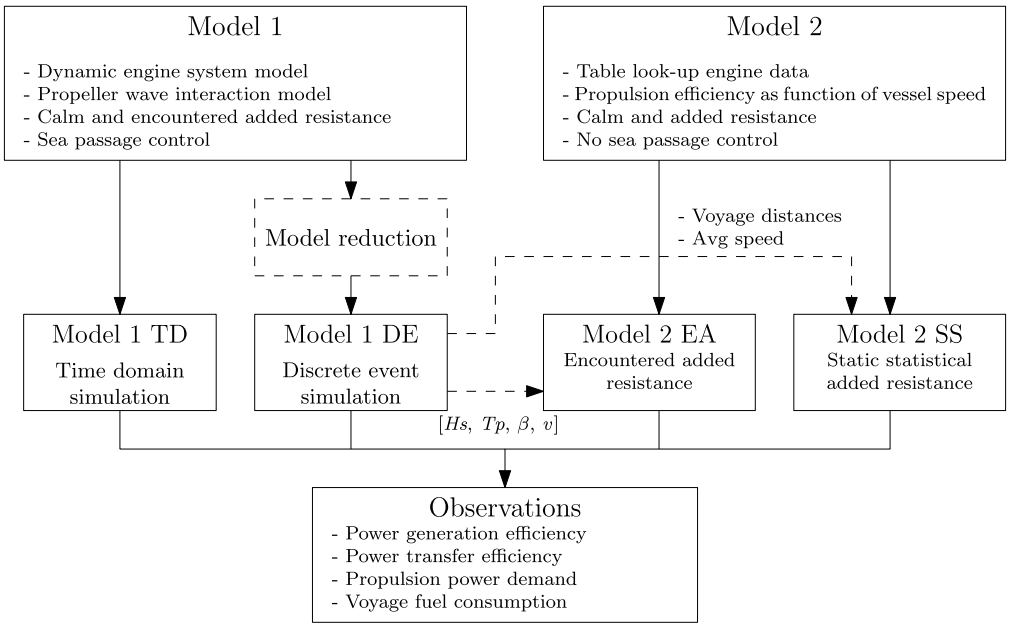

Fig. 7. Models and model implementations compared and evaluated in the case study. Additional information required by the Model 2 implementations are provided by Model 1 simulation results.

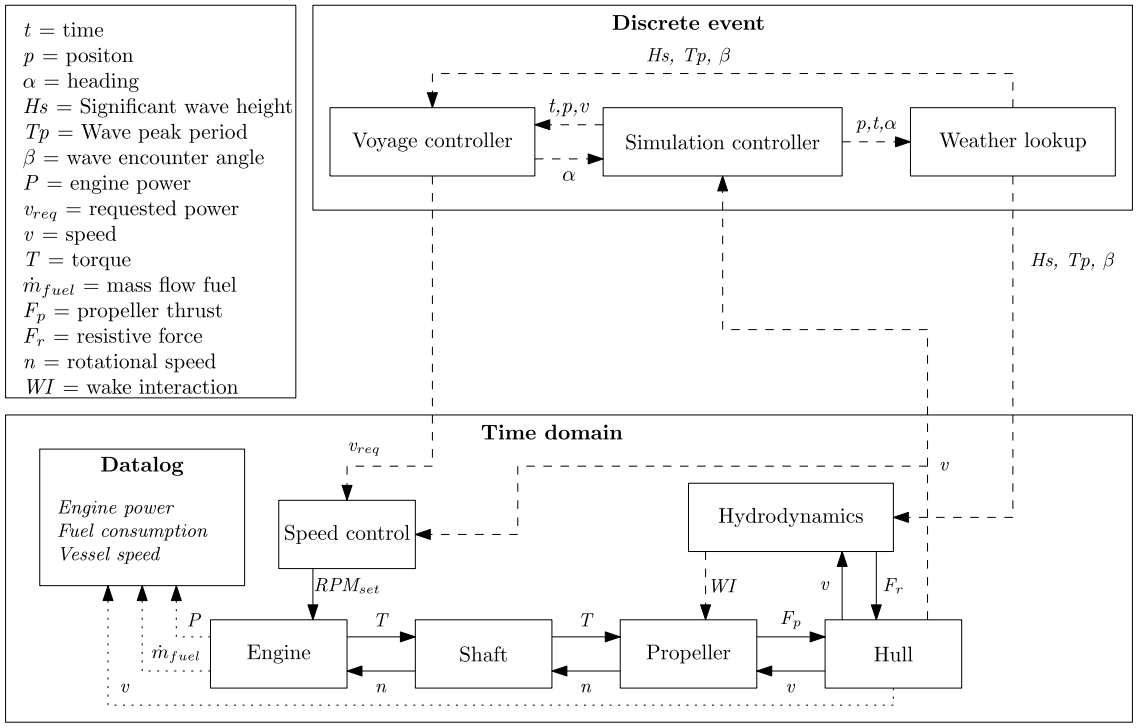

Fig. 8. Overview Model 1 time domain vessel model and discrete event voyage and weather controller.

the problem of estimating fuel consumption to a problem where the only needed inputs are vessel speed and voyage distance. To enable comparison of model fidelities and not route selection, the average vessel speeds and voyage distances from Model 1 is used as input to Model 2.

3.2. Sea passage scenarios

The sea passage sub-model has been used to include three sea passage scenarios with V_0 and κ values as presented in Table 1. The scenarios have been designed to represent different operation policies. The Low Cost Low Velocity (LCLV) scenario parameters are determined to allow speed and route variation, which is expected to result in a low engine power demand. High Cost Low Velocity (HCLV) is a scenario where the arrival time is stricter than for LCLV, however the low target speed is likely to limit the need for high power demands for the majority of the time. The High Cost High Velocity (HCHV) is set to test the fuel consumption and power estimates at a likely high power demand scenario. The three cases span the majority of the relevant engine loading range, allowing us to investigate the influence of model fidelity on estimates at different engine load intervals. As seasons affect prevailing weather conditions, and consequently the operational sea

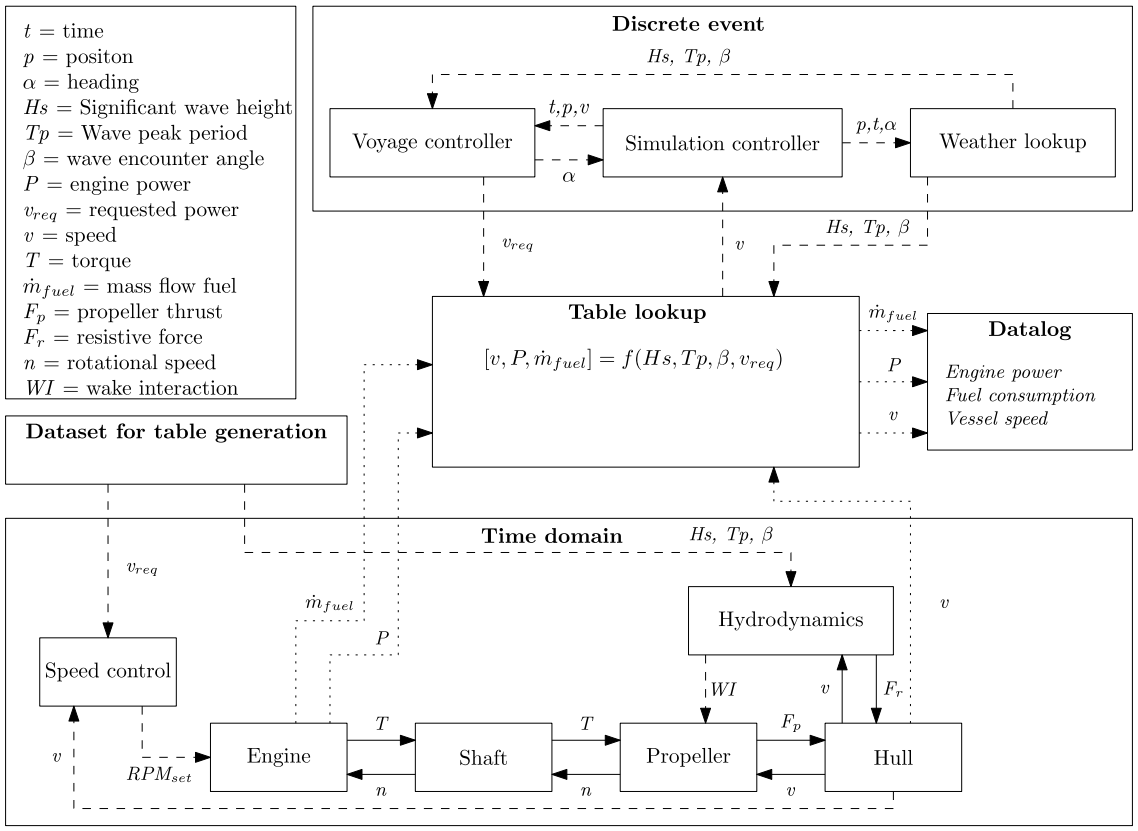

Fig. 9. Overview Model 1 discrete event vessel model and discrete event voyage and weather controller, with information on model reduction from the time domain model.

Table 1
Sea passage scenarios.

	LCLV	HCLV	HCHV
V_0 [kn]	14	14	15
κ [tons/h]	4	7	10

state conditions, it was selected to include all seasons in the case study. Twelve voyage start dates were selected with historic weather data from 2016. The start dates are the 2. for each month of the year. Table 1 lists the input parameters describing the operational scenarios used in the case study.

3.3. Simulation

Two simulation methods are compared in the case study, time domain and discrete event. Model 1 is simulated in both time domain and in discrete event, while Model 2 is only simulated in discrete event. Using Model 1 in a discrete event simulation requires reducing the dynamic model into a table look up model. While such a model reduction can reduce the result validity, it contributes to a significant simulation speed increase. Fig. 7 shows the different implementation of the different models both with regard to simulation method and information flow from model 1 to model 2.

3.3.1. Time domain simulation

The complete voyage is simulated using Model 1 in the time domain with discrete updates of sea states and ship control inputs based on the sea passage controller presented in Section 3.1.1. The combination of the discrete event sea passage model and Model 1 is presented in Fig. 8. The voyage controller determines the required speed which is used as a set-point to a vessel speed controller setting the engine RPM. At discrete times, the weather is updated by the weather look-up module. Weather

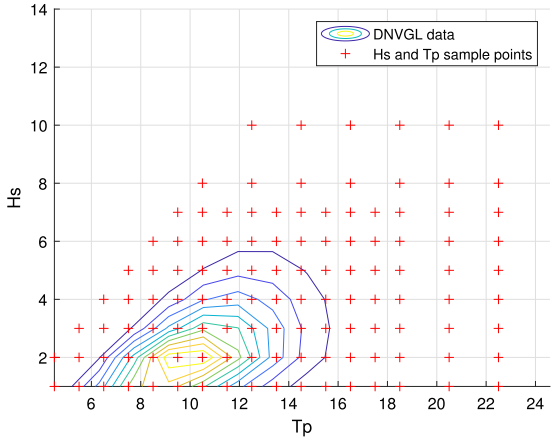

Fig. 10. Sampling pattern for table look-up Tp Hs combinations based on the DNVGL wave scatter data (DNVGL, 2017) represented by a contour plot.

is given as an array of Hs, Tp, and encounter angle to calculate hull resistance and propeller performance.

3.3.2. Discrete event simulation

A discrete-event formulation is used to replicate the voyage utilizing the sea passage controller and a table look-up representation of the dynamic model. The process of generating the table look-up and running the simulation is presented in Fig. 9. The table look-up model is generated before the voyage simulation by running the time domain simulation model for a selection of sea states, encounter headings and vessel speeds. This generates a matrix of engine performance as a function of Hs, Tp, encounter angle and requested vessel speed. Time domain simulations for the table generation are run until steady state

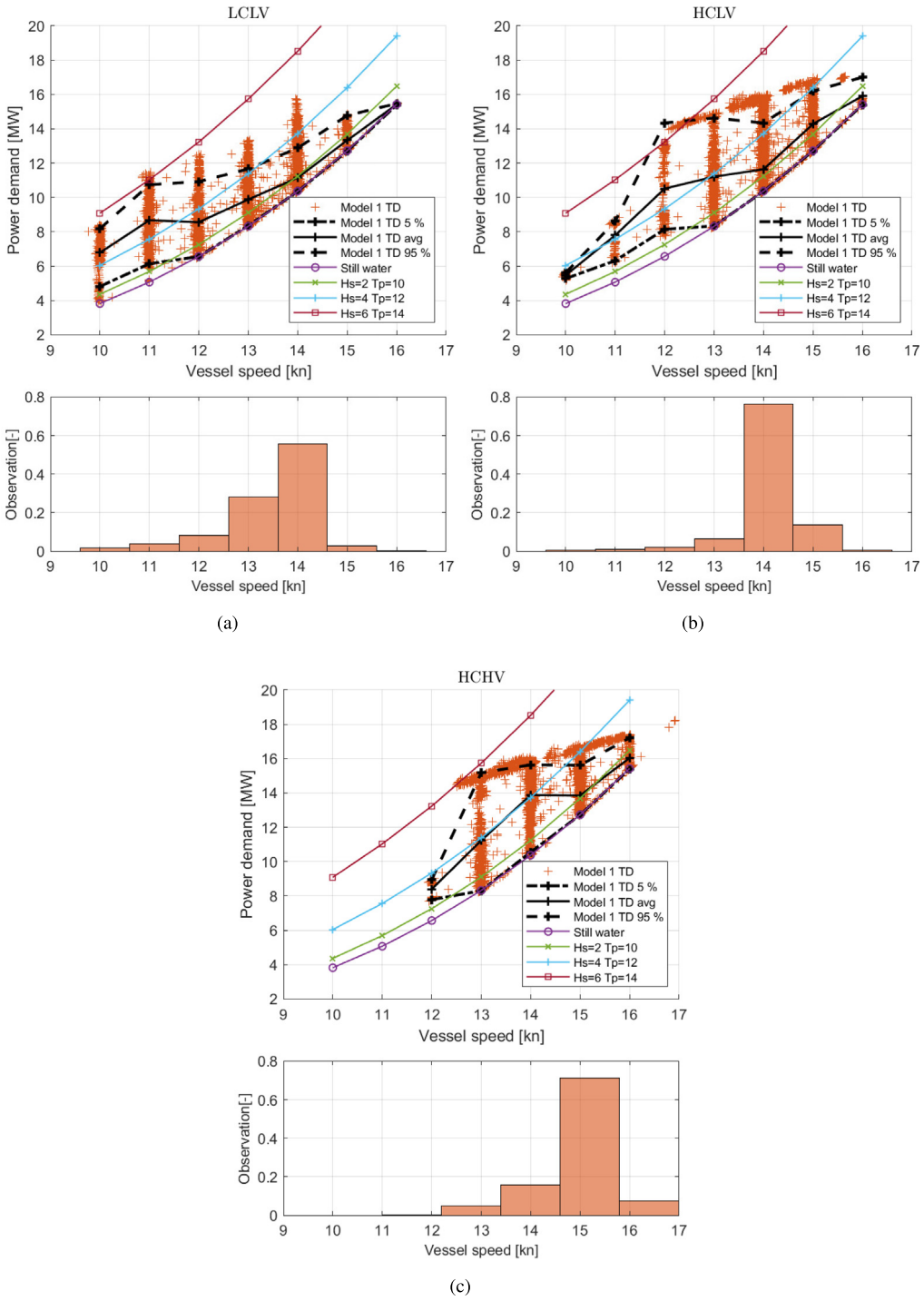

Fig. 11. Comparison of still water power demand and power demand observed in Model 1 TD simulation results for the three sea passage scenarios. A 90% confidence interval and average is added to providing insight into distribution of observations.

operation is achieved. Linear interpolation is used to estimate power system performance of the encountered sea states during the voyage. During the voyage simulation, calls to the table look-up module are the same as for the time domain model.

Headings and engine speeds ranged from 65 rpm to the maximum rpm of 95 and headings from 0 to 180 degrees with 45 degree increments. Wave conditions are presented in Fig. 10, where Hs and Tp combinations are based wave scatter data from DNVGL (2017). In addition to covering the most likely Hs and Tp combinations, some extreme values are also included to remove the need for extrapolation in extreme weather situations. Total number of simulation runs for generation of table look-up matrix became 6435.

4. Results

In this section, results of the case study are presented. First, a base line for comparison using Model 1 time domain simulation results is presented for power demand, power transmission, power production and fuel consumption. Then, a comparison of how the two base models and three of the model implementations, Model 1 TD and DE and Model 2 EA, will be compared with regards to effect of model fidelity. Lastly,

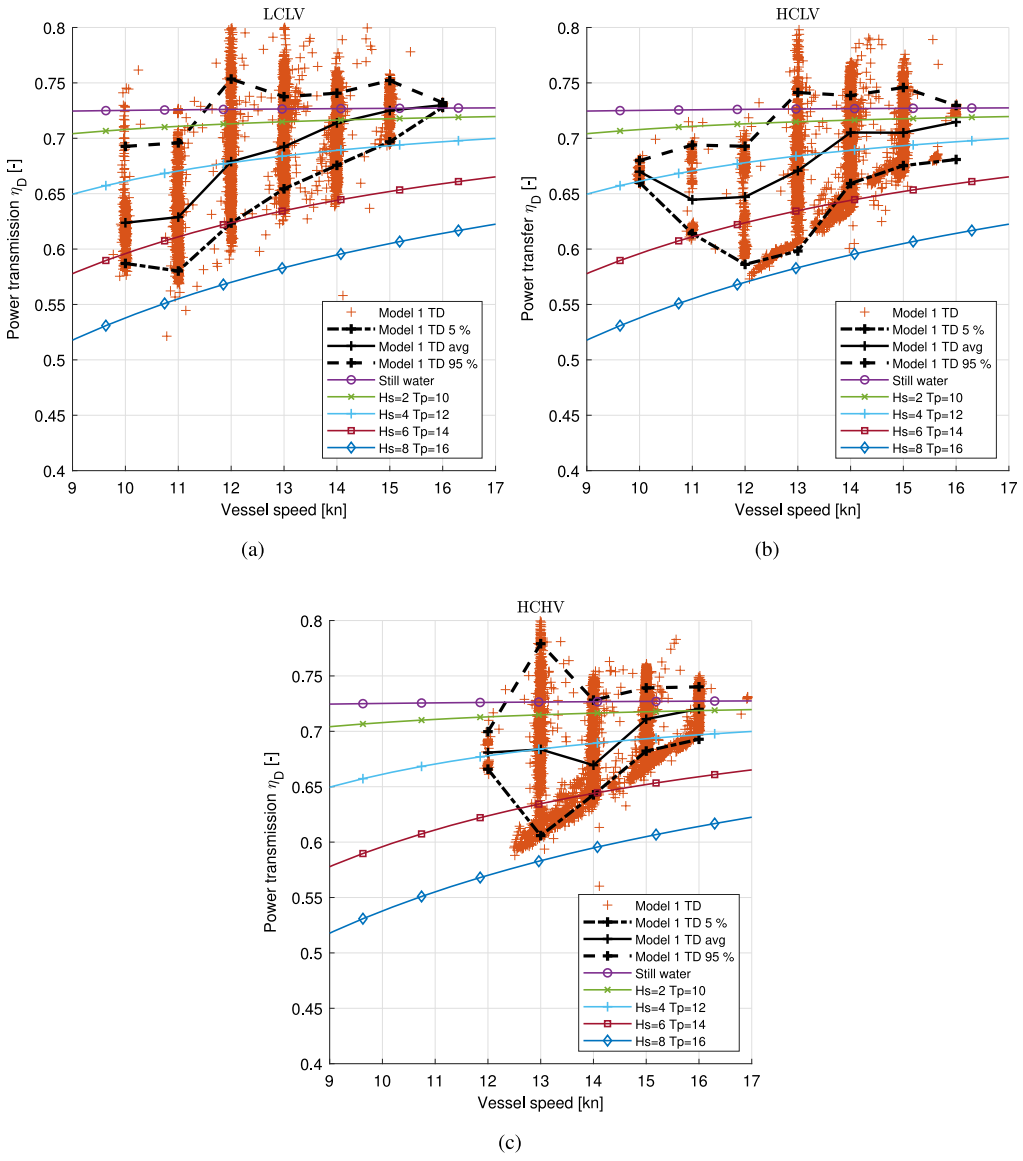

Fig. 12. Comparison of still water propulsion efficiency and propulsion efficiency observed in Model 1 TD simulation results for the three sea passage scenarios. A 90% confidence interval and average is added to providing insight into distribution of observations.

a comparison of all the models and model implementations is presented where predictions on total fuel consumption and fuel consumption per sailed distance are evaluated.

4.1. Factors affecting fuel consumption estimation

4.1.1. Power demand

Power demand has been evaluated as function of vessel speed. The comparison is presented in Fig. 11, where the LCLV sea passage scenario is found in Fig. 11(a), HCLV in Fig. 11(b) and HCHV in Fig. 11(c). The scatter data is augmented with an average and a 90% confidence interval for power demand within seven vessel speeds intervals based on empirical distributions. Estimated power demand for a selection of sea states assuming head waves is included for reference.

The same load dynamics and speed transients can be observed in the power demand data as scatter points outside the requested speeds. In addition to the grouping on the voyage controller requested speeds and random scattering due to transients there are observable lines of scatter points between the speed groupings at high power demand. These lines are observable in both the HCLV and HCHV sea state scenarios. These scatter points are caused by involuntary speed loss, where the engine and propeller are not able to deliver enough thrust to overcome the resistance for a required speed. As with the propulsion efficiency, the lowest errors are found at and above the vessel speed with the highest number of observations.

4.1.2. Power transmission

The power transmission efficiency has been evaluated as function of vessel speed. Observed efficiencies in the simulation results for the different sea passage scenarios are compared to efficiency curves for different wave conditions assuming head waves. The comparison is plotted in Fig. 12, where data for the LCLV scenario is given in Fig. 12(a), the HCLV scenario in Fig. 12(b) and the HCHV scenario in Fig. 12(c). The scatter data from the time domain simulation of Model 1 is augmented with an average and a 90% confidence interval for propulsion efficiency with seven vessel speeds intervals based on empirical distributions. In addition the distributions of observed vessel speeds is included in a histogram for each sea passage scenario. These vessel speed observations and distributions are applicable to all data presented with vessel speed at the x-axis in Section 4.1. In the scatter plot, observations are grouped around speeds set by the voyage controller which have a 1 knot resolution. There are also some

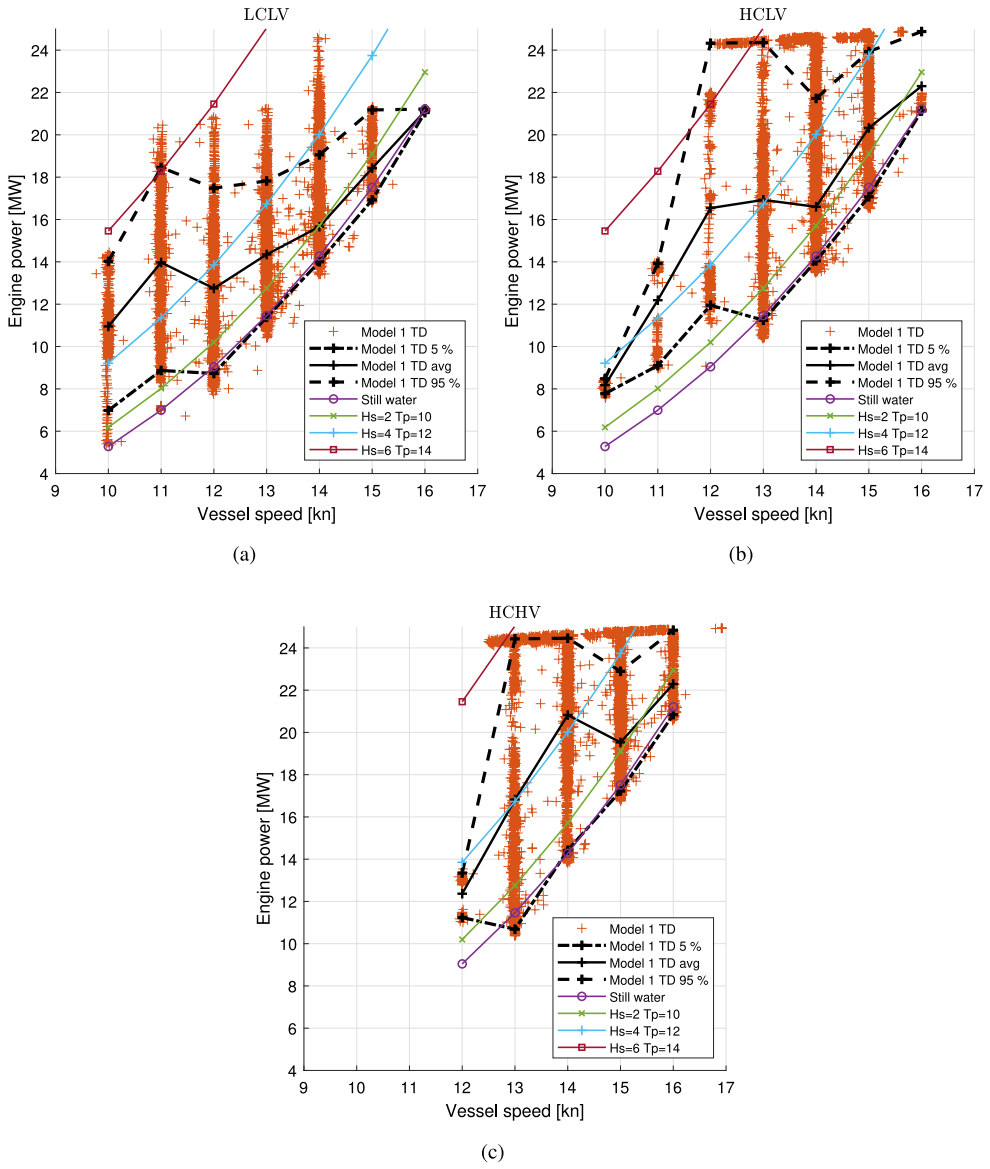

Fig. 13. Combining the propulsion efficiency and the power demand to produce the required engine power. Data based on observations from Model 1 TD simulation results for the three sea passage scenarios. A 90% confidence interval and average is added to providing insight into distribution of observations.

observations in between the requested speeds and below and above the expected band of propulsion efficiency. This is due to the dynamic load and transients between requested speeds and the way propulsion efficiency is calculated. Propulsion efficiency is calculated based on the engine power divided by the power demand. In situations where the engine power drops rapidly, the inertia of the ship causes a much slower vessel speed reduction. This results in an increased propulsion efficiency as the power demand is virtually unchanged in the time it takes for the engine power to drop significantly. When comparing the error between a calm water propeller performance as function of speed, and the observed efficiencies with the distribution of observations in relation to vessel speed, we find that the errors are at its smallest at and above the vessel speeds with the highest number of observations.

4.1.3. Power production

Combining the power demand and propulsion efficiency gives the required engine power. The engine power scatter data is presented as function of vessel speed in Fig. 13, with sea passage scenario LCLV in Fig. 13(a), HCLV in Fig. 13(b) and HCHV in Fig. 13(c). The scatter data is augmented with an average and a 90% confidence interval for engine power within seven vessel speeds intervals based on empirical distributions. The estimated engine powers for a selection of sea states assuming head waves and propulsion efficiency a function of propeller speed and vessel velocity are included for reference. As with the propulsion efficiency and power demand, the lowest errors are found at and above the vessel speed with the highest number of observations.

4.1.4. Fuel consumption

As the main performance indicator used in this case study is fuel consumption per sailed distance, a fuel consumption plot comparable to those of the factors influencing fuel consumption is presented in Fig. 14. Sea passage scenario LCLV is presented in Fig. 14(a), HCLV in Fig. 14(b) and HCHV in Fig. 14(c). The scatter data is augmented with an average and a 90% confidence interval for fuel consumption within 7 vessel speeds intervals based on empirical distributions. Estimated fuel consumption for a selection of sea states assuming head waves based on a test-bench propeller curve engine efficiency is also included to enable evaluation of the importance of encountered sea states on the fuel consumption.

The involuntary speed loss scatter data line is also observed in the fuel consumption plots. Here, the line shows an increase with reduced

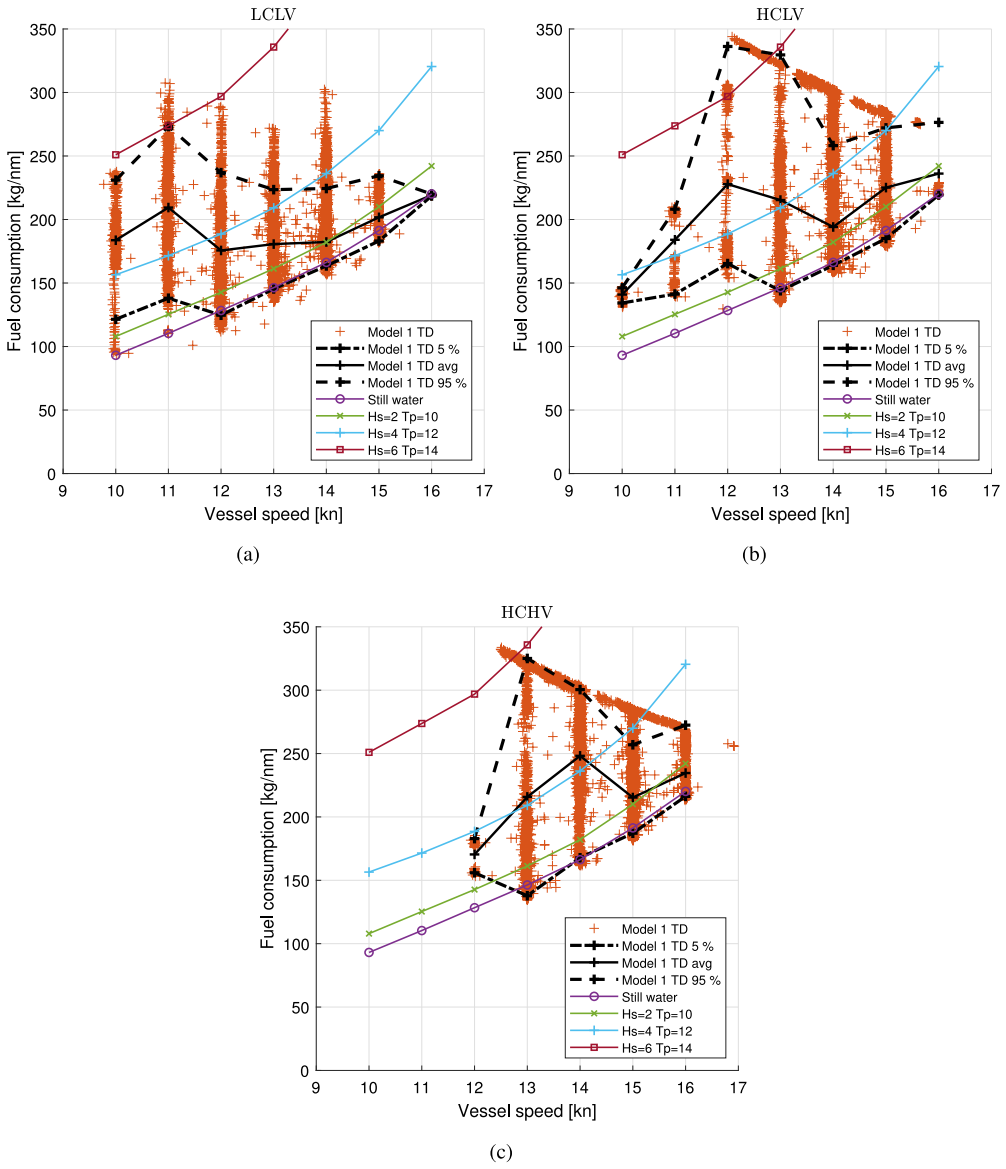

Fig. 14. Combining engine power demand, vessel speed and specific fuel consumption to produce fuel consumption per sailed distance. Data based on observations from Model 1 TD simulation results for the three sea passage scenarios. A 90% confidence interval and average is added to providing insight into distribution of observations.

speeds which is expected as the engine power is constant giving the same fuel consumption per time unit while the distance covered is reduced. Comparing still water fuel consumption with observed fuel consumption in the simulation results highlight a significant discrepancy. As with the propulsion efficiency, power demand and engine power, the lowest errors are found at and above the vessel speeds with the highest number of observations.

4.1.5. Specific fuel consumption

Specific fuel consumption [g/kWh] is a common way of evaluating power production efficiency. The effect of operational conditions of specific fuel consumption and engine power distribution is compared for the three sea passage scenarios. The comparison is plotted in Fig. 15, where data for the LCLV scenario is given in Fig. 15(a), the HCLV scenario in Fig. 15(b) and the HCHV scenario in Fig. 15(c). The scatter data from the time domain simulation of Model 1 is augmented with an average and a 90% confidence interval for specific fuel consumption values within 16 engine power intervals based on empirical distributions. Engine power distributions of observed engine power are included in a histogram for each sea passage scenario.

4.2. Comparing model fidelities

In this section a comparison of the average and the 90% confidence interval for Model 1 TD, Model 1 DE and Model 2 EA is carried out. Observations for all sea passage scenarios are combined to generate the underlying data sets. Fig. 16 compares the observed specific fuel consumption. As Model 2 is based on the engine test-bench propeller curve there is no confidence interval. In addition to the comparison of specific fuel consumption distributions for the different models, a histogram representing the observed engine powers for all sea passage scenarios is also included. Fig. 17 compares propulsion efficiency 17(a), power demand 17(b), engine power 17(c) and fuel consumption per sailed distance 17(d). Fig. 17(a) also includes the vessel speed observation distributions for all scenarios combined. There are only vessel distributions available for Model 1 TD and Model 2 DE. Model 2 EA vessel speeds are based on the vessel speeds of Model 1 DE.

The time series of different performance indicators for the voyage simulations with departure in March are included in Fig. 18 as an example of how the different models deviate at low load and high load during a voyage. An accompanying data set presenting the voyage and

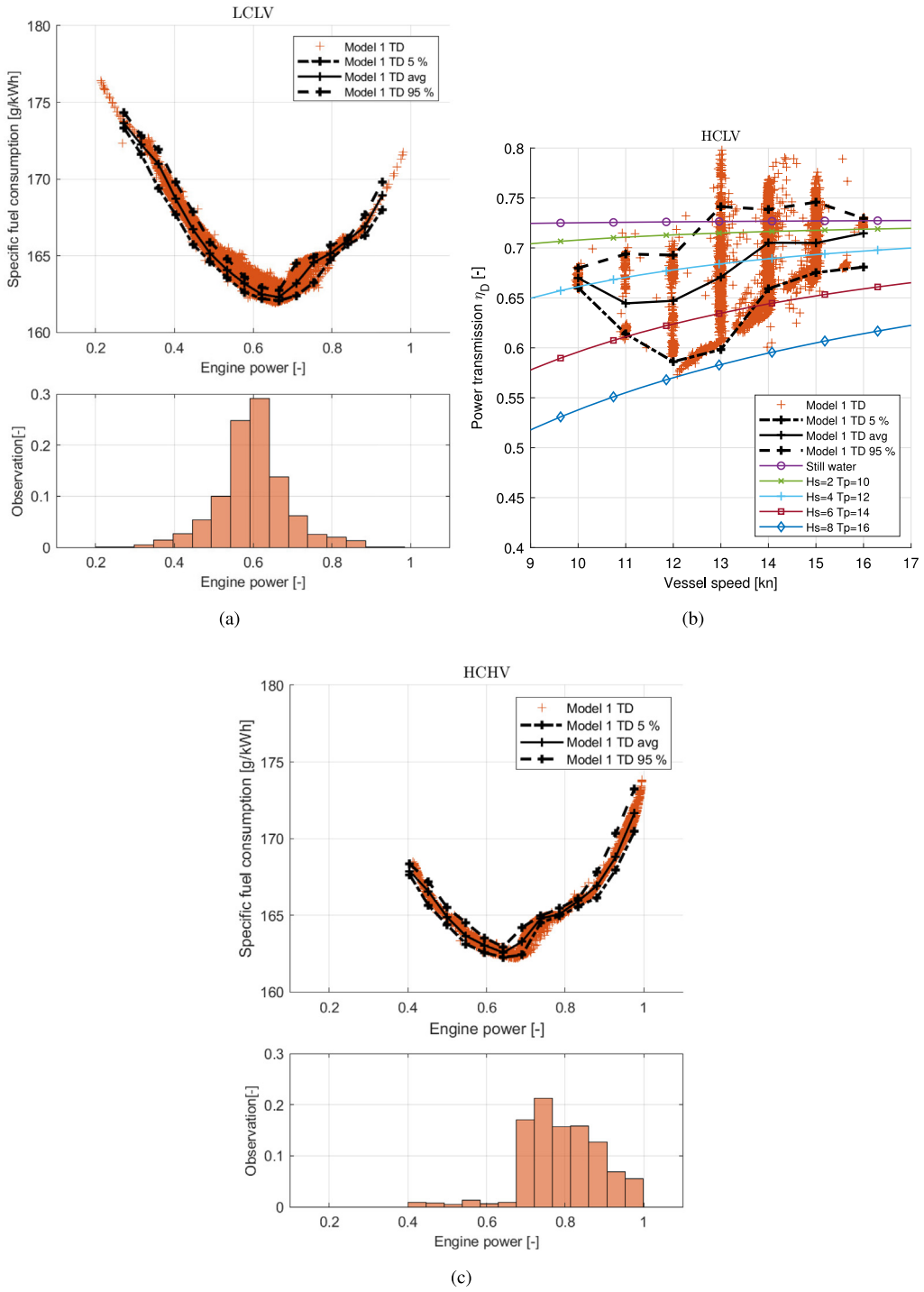

Fig. 15. Comparison of engine SFOC observed in Model 1 TD simulation results for the three sea passage scenarios. A 90% confidence interval and average is added to providing insight into distribution of observations. In addition distribution of observations regarding engine power is plotted as a histogram.

sea states encountered is presented in Fig. 19, where Model 2 is based on the voyage of Model 1 DE.

4.2.1. Comparing time domain and discrete event voyage simulation

Time series for Model 1 TD and Model 1 DE for all three March sea passage scenarios are presented in Fig. 19, where data for the voyage controller output and resulting route with encountered operational conditions are presented. The voyage control data are vessel speed and course settings. Data on encountered operational conditions are included in the form Hs and positions in the form of latitudes and longitudes. In addition there are two plots comparing Model 1 TD and DE by plotting differences in speed and course between the two models.

The spikes observed in the speed difference plot are due to the speed transients occurring in Model 1 TD. Changing vessel speed in the TD model by one knot takes about 15 min, while it is instant in the DE model. There are no dynamics in the course changes so spikes observed in the course difference chart are due to differences in temporal resolutions and the exact time of course change. It can be observed that

Table 2
Voyage particulars, sailed distance and average speed.

	Sailed distance [nm]						Average vessel speed [kn]					
	LCLV		HCLV		HCHV		LCLV		HCLV		HCHV	
	TD	DE	TD	DE	TD	DE	TD	DE	TD	DE	TD	DE
jan	4287	4290	4282	4356	4297	4314	13.0	13.0	13.9	14.0	14.3	14.4
feb	4325	4374	4336	4404	4329	4404	13.0	13.0	14.1	14.1	14.7	14.7
mar	4342	4374	4317	4362	4296	4348	13.5	13.5	14.0	14.0	14.8	14.8
apr	4394	4458	4323	4408	4313	4365	12.9	12.8	14.1	14.1	14.5	14.5
mai	4282	4368	4284	4284	4283	4332	13.7	13.5	14.0	14.0	15.0	15.0
jun	4282	4362	4280	4284	4282	4314	13.7	13.7	14.0	14.0	15.0	15.0
jul	4281	4314	4283	4290	4282	4320	13.8	13.8	14.0	14.0	15.0	15.0
aug	4296	4338	4290	4374	4286	4320	13.8	13.6	14.0	14.0	15.0	15.0
sep	4281	4362	4280	4284	4282	4320	14.0	13.7	14.0	14.0	15.0	15.0
okt	4405	4410	4395	4403	4434	4409	13.4	13.4	14.4	14.4	14.6	14.4
nov	4423	4512	4525	4569	4338	4427	12.7	12.7	13.6	13.6	14.8	14.8
des	4291	4356	4284	4368	4288	4326	13.6	13.4	14.0	14.0	15.0	15.0
avg	4324	4377	4323	4366	4309	4350	13.4	13.3	14.0	14.0	14.8	14.8
diff	–	52	–	42	–	41	–	−0.1	–	0.0	–	0.0
diff %	–	1.21%	–	0.98%	–	0.95%	–	−0.49%	–	0.05%	–	−0.10%

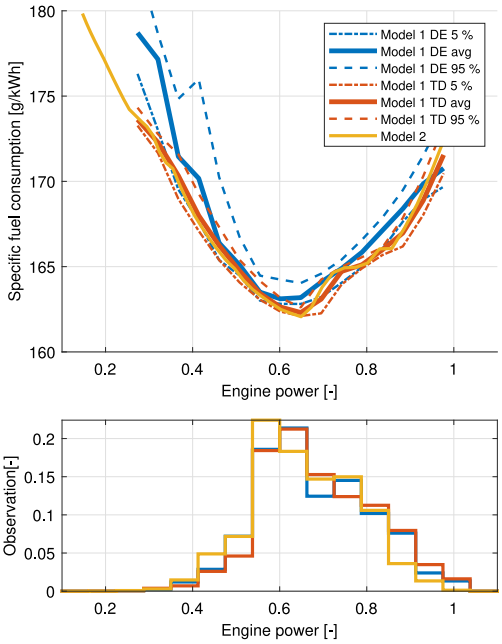

Fig. 16. Comparison of specific fuel consumption curves between the different model implementations for operational conditions.

the differences in speed policy and route occur towards the end of the voyage and that the two models handle speed loss differently in some instances. Data for all voyages and all sea passage scenarios in the form of sailed distances and average speed are presented in Table 2.

4.2.2. Operational performance prediction

The operational performance in this case study is based on fuel consumption, either total fuel consumed during a voyage or the fuel consumption per sailed distance. Total fuel consumption for the voyages are presented in Table 3. Model 2 SS is also included, although the method is not intended for use on a single voyage. This is due to the estimated power demand being based on static statistical approach, meaning that it is only appropriate to compare the sum over a year as it is not relevant for single voyages. Average fuel consumption per sailed distance is presented in Table 4, where the total fuel consumption for a voyage is divided by the distance sailed.

5. Discussion

Up to this point we have presented model details, case specifics and simulation results. In this section, we discuss the meaning of the results and potential implications of the findings. As this case study has been carried out for a large VLCC-tanker, all observations made may not be applicable to other types of vessel. Other results may also be expected for other types of vessels, such as container ships operating at higher speeds with cargo that are more susceptible to damage and slenderer hulls that behaves differently in waves. However, the considerations on how operational performance prediction both depends on models used and how the evaluation is carried out, are relevant for all ship categories.

5.1. The influence of the different factors affecting fuel consumption estimates

From the time domain simulation results it is evident that operation in waves has an impact on estimating the fuel consumption. However, the impact varies for the different factors. The effect of operation in waves and transients have some impact on engine specific fuel oil consumption, however the difference is very small compared to the still water specific fuel oil consumption. Power transmission does however have a significant impact on fuel consumption in waves, which can be seen in Table 3 comparing Model 1 DE and Model 2 EA. In waves the power transmission efficiency changes significantly from that of still water operation, which affect both the required engine power and at which specific fuel consumption the power is produced. Although all models use the same estimate for still water resistance and added resistance due to waves, it is evident that the method of including waves into the estimation has a significant effect of fuel consumption estimation when comparing the total fuel consumption of Model 2 EA and Model 2 SS in Table 3.

5.2. Model comparison

In comparing the models, Model 1 TD functions as the reference. The main difference between Model 1 and Model 2 is that Model 2 requires input on encountered operational conditions and voyage particulars. In this case study these data have been provided by Model 1 DE to ensure that the model comparisons are based on the same voyages. However, additional differences between the models are expected if other methods for estimating voyages are used for creating the required input to Model 2 (Sandvik et al., 2018). In this section, mainly Model 1 TD, Model 1 DE and Model 2 EA are compared, as Model 2 SS only produces data relevant when comparing fuel consumption over a year.

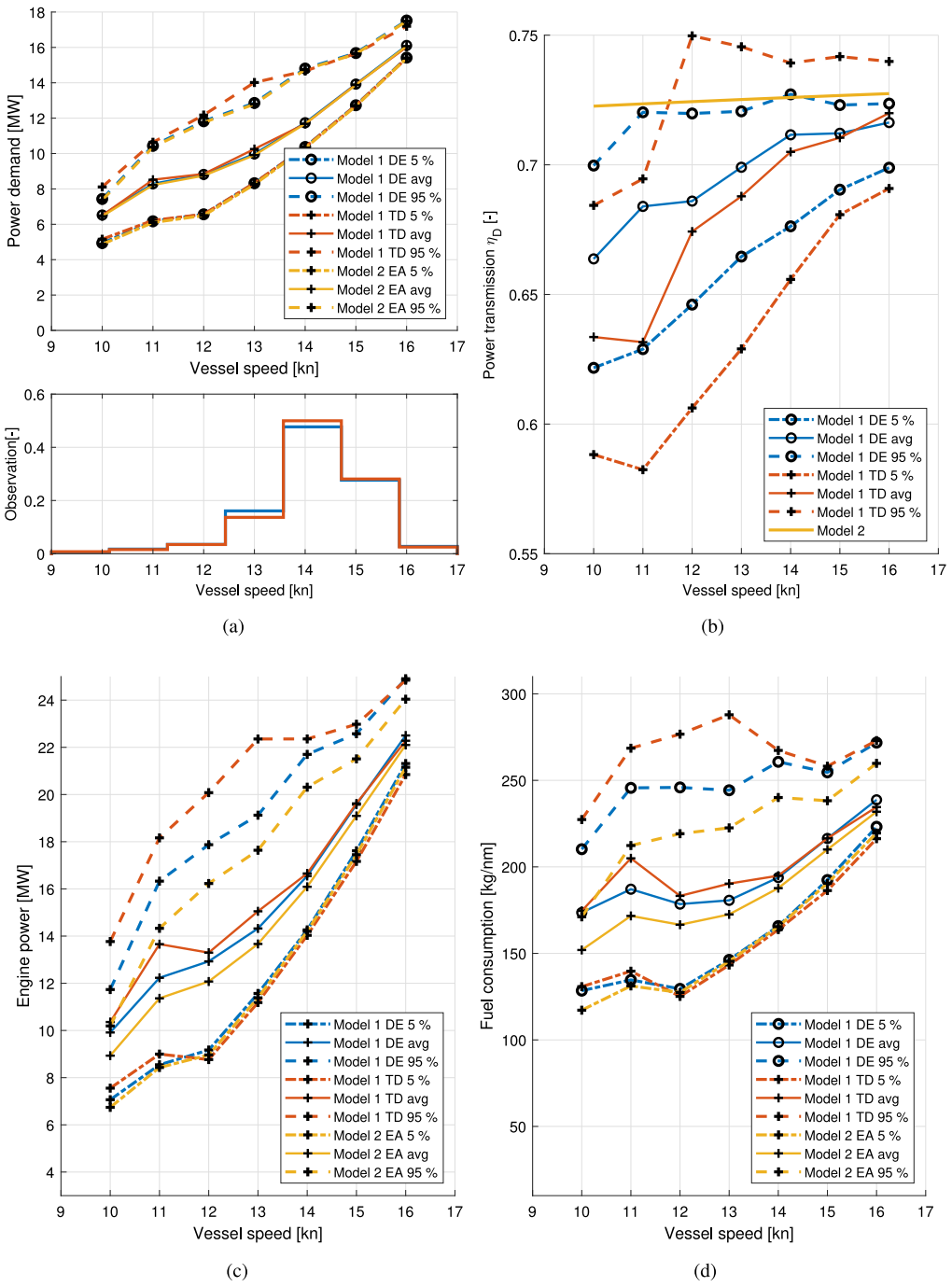

Fig. 17. Combining engine power demand, vessel speed and specific fuel consumption to produce fuel consumption per sailed distance. Data based on observations from Model 1 TD simulation results for the three sea passage scenarios. A 90% confidence interval and average is added to providing insight into distribution of observations.

Important reasons for the observed differences between Model 1 TD and DE, are the errors introduced in both the curve fitting needed to create the table lookup model and the linear interpolation performed to estimate performance. Errors in curve fitting are especially evident in the estimation of the specific fuel consumption in Fig. 16. These errors are limited in the estimation of power demand, see Fig. 11, while they are observable in both estimation of propulsion efficiency, see Fig. 12, engine power, see Fig. 13, and fuel consumption per sailed distance, see Fig. 14. However, the differences are not significant in the operation points which have the bulk of observations, see the histogram in Fig. 12. The result is that the overall differences between Model 1 TD and DE are small when comparing total fuel consumption or fuel consumption per sailed distance, see Tables 3 and 4. Another source of difference between Model 1 TD and DE is the effect of accumulating difference in the sailed route due to speed change transients and difference in estimating speed loss. In this case study, transients when changing speed take about 1000 s, which results in a difference in position. In addition, the DE model uses simplified estimates for speed loss while speed loss of the TD model is part of the simulation. If the difference gets large, or the differences in cost estimates for different route alternatives are small, this can result Model 1 TD and DE sailing different routes. This effect gives a bias when using the TD model as the performance estimate of the voyage controller is not equal to what the ship does. The effect of this bias would become more pronounced for longer voyages.

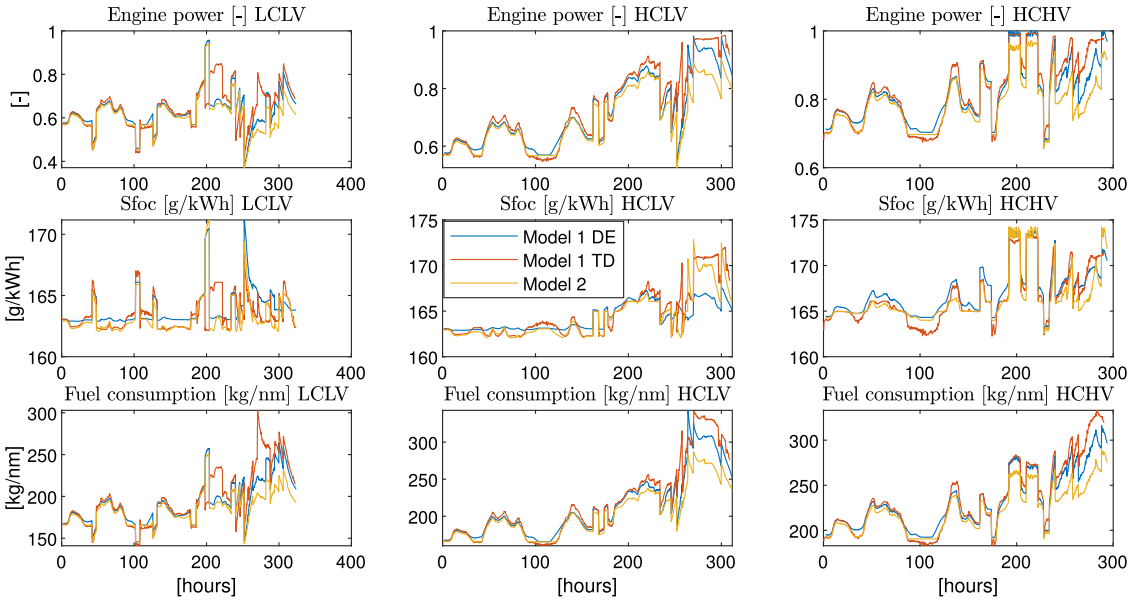

Fig. 18. Model 1 TD, Model 1 DE and Model 2 time series for the voyage simulations with departure in March with performance data for LCLV, HCLV and HCHV sea passage scenarios.

Table 3
Comparison of model estimated operational performance given as total fuel consumption.

	Total fuel consumption [1000 kg]											
	LCLV				HCLV				HCHV			
	TD	DE	EA	SS	TD	DE	EA	SS	TD	DE	EA	SS
jan	812.7	800.4	758.3	720.6	933.4	939.7	885.6	816.9	1016.0	1003.6	945.0	858.0
feb	743.2	743.0	724.3	736.2	898.0	896.2	869.5	842.9	978.3	979.5	946.8	910.8
mar	849.4	837.9	807.3	777.8	935.5	926.2	886.9	819.8	1000.4	1003.5	963.7	910.6
apr	802.4	790.3	759.2	732.7	995.5	988.7	941.9	845.2	1058.7	1055.4	992.1	888.4
mai	760.4	754.3	735.0	775.1	792.8	788.1	768.6	807.0	918.6	931.6	902.2	932.0
jun	741.7	752.1	739.4	795.1	774.3	768.7	755.3	807.0	898.7	899.7	880.0	921.8
jul	747.1	748.3	738.2	796.5	761.5	758.5	748.4	810.3	865.8	877.6	861.1	925.2
aug	753.0	739.5	728.5	783.9	774.3	783.4	770.7	826.2	893.3	896.0	877.1	925.2
sep	725.1	716.5	710.7	795.1	726.8	728.1	722.6	807.0	853.0	866.4	852.6	925.2
okt	856.9	837.7	802.6	772.3	943.2	961.6	918.6	877.2	1018.7	1083.1	999.0	880.7
nov	922.9	917.4	858.2	736.2	1027.7	1024.6	957.2	821.5	990.7	1002.0	963.7	924.1
des	763.6	759.0	739.2	769.8	823.2	830.0	808.6	822.8	962.2	964.8	934.2	928.6
sum	9478	9396	9101	9191	10386	10394	10034	9904	11454	11563	11118	10930
diff	–	−82	−377	−205	–	8	−352	−490	–	109	−337	−633
diff %		−0.87%	−3.98%	−2.18%		0.07%	−3.39%	−4.71%		0.95%	−2.94%	−5.47%

Table 4
Comparison of model estimated operational performance given as specific fuel consumption per sailed distance.

	Specific fuel consumption pr nautical mile [kg/nm]											
	LCLV				HCLV				HCHV			
	TD	DE	EA	SS	TD	DE	EA	SS	TD	DE	EA	SS
jan	189.6	186.6	176.8	168.0	218.0	215.7	203.3	187.5	236.4	232.7	219.1	198.9
feb	171.8	169.9	165.6	168.3	207.1	203.5	197.4	191.4	226.0	222.4	215.0	206.8
mar	195.6	191.6	184.6	177.8	216.7	212.3	203.3	187.9	232.9	230.8	221.7	209.4
apr	182.6	177.3	170.3	164.4	230.3	224.3	213.7	191.7	245.5	241.8	227.3	203.5
mai	177.6	172.7	168.3	177.5	185.1	184.0	179.4	188.4	214.5	215.0	208.3	215.1
jun	173.2	172.4	169.5	182.3	180.9	179.4	176.3	188.4	209.9	208.6	204.0	213.7
jul	174.5	173.5	171.1	184.6	177.8	176.8	174.5	188.9	202.2	203.2	199.3	214.2
aug	175.3	170.5	167.9	180.7	180.5	179.1	176.2	188.9	208.4	207.4	203.0	214.2
sep	169.4	164.3	162.9	182.3	169.8	170.0	168.7	188.4	199.2	200.6	197.4	214.2
okt	194.6	190.0	182.0	175.1	214.6	218.4	208.6	199.2	229.8	245.6	226.6	199.7
nov	208.7	203.3	190.2	163.2	227.1	224.3	209.5	179.8	228.4	226.3	217.7	208.7
des	177.9	174.3	169.7	176.7	192.2	190.0	185.1	188.4	224.4	223.0	216.0	214.6
avg	182.7	178.9	173.3	175.0	200.2	198.4	191.5	187.7	221.5	221.5	213.0	209.4
diff %	–	−2.09%	−5.41%	−4.37%	–	−0.91%	−4.52%	−6.64%	–	0.00%	−4.01%	−5.79%

When comparing Model 1 and 2, it is most relevant to compare Model 1 DE and Model 2 EA as the EA model uses the same route as the DE model. The use of still water specific fuel consumption curve with fuel consumption as function of engine power in Model 2 EA,

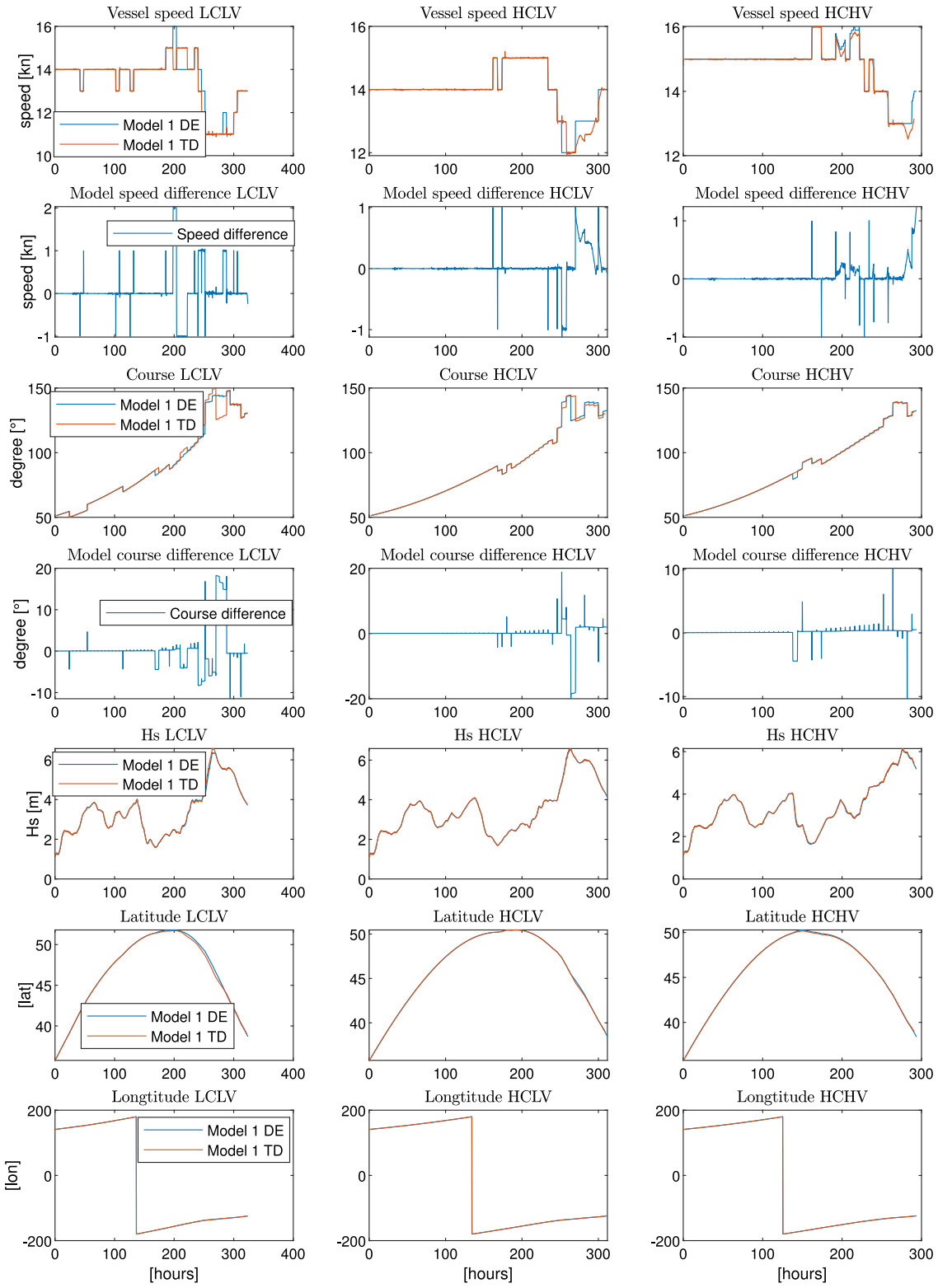

Fig. 19. Model 1 TD and Model 1 DE time series for voyage simulations with departure in March with data for LCLV, HCLV and HCHV sea passage scenarios. Deviating voyages both with regards to speed and course are observable. Difference in involuntary speed loss is also observed.

is based on the data in Fig. 16 a reasonable assumption. Time series for the voyages carried out in March seen in Fig. 18, show that this assumption is reasonable as the specific fuel consumption curve of Model 2 EA have less deviation from Model 1 TD than Model 1 DE. However simplifying the propulsion efficiency to a function of speed only introduces significant differences compared to Model 1 DE as seen in Table 3. This simplification leads to a significant shift in the peak of the observed engine powers seen in Fig. 15.

Another area of comparison of the different models is the required modelling and simulation effort. Model 1 is based on high fidelity models of the engine system, propulsion system, hull and hydrodynamics. Such models are time consuming to develop and require significant

amount of information that is challenging to obtain, especially in an early design phase (Tillig et al., 2018). The simulation effort, both for the time domain model and the model reduction, is significant compared to the fast calculations required for Model 2. Currently, it is common to use the approach of Model 2 in higher level estimations of operational performance applications such as weather routing (Zaccone et al., 2018), voyage optimization (Lu et al., 2015), bottom-up emission estimation (Kilic and Tzannatos, 2014). In these cases, where the goal is just to evaluate an already available system where data is easily available, engine models, such as the still water specific fuel consumption curve of Model 2, are reasonable. In this work, the focus is however on operational performance evaluation in the context of evaluating novel system design solutions. While the goal is to always use as simple models as possible while still capture the effect of design changes, it might not be achievable to use simple models, such as Model 2. For more advanced systems designed to satisfy EEDI requirements, including PTI/PTO, waste heat recovery, emission abatement etc., a still water specific fuel consumption curve may not adequately describe the system performance at all times. Other aspects that need to be taken into account is whether the system performance is dependent on the history of the system, or if it is by all practical considerations only dependent on a very short history. A diesel engine has time constants dictated by the turbo charger and thermal transients, however these time constants are very short compared to a voyage and can in most cases be ignored. A hybrid system with energy storage based on batteries have longer time constants, and is thereby dependent on a longer history which may affect decision making and performance.

6. Conclusions

The case study designed to evaluate four ship system model fidelity levels for operational performance uncovered that model fidelity affected results both due to differences in how different factors had been modelled and how the different models were simulated. The main factor affecting performance in operational conditions was found to be the propulsion efficiency estimation. Dynamic operation of the marine power system was investigated and found to be of less importance when estimating operational performance. The difference between Model 1 TD and DE was found to be negligible considering the significant simulation effort required for the TD model compared to the DE model. However model fidelity required does not only depend on the ability to provide useful prediction, it also depends on the availability of information that can be used for less simulation intensive models. This is illustrated in the case study where all models rely on information from Model 1 TD for model development through model reduction to either a table lookup model or for the still water specific fuel consumption curve.

Acknowledgements

This work was carried out at SFI Smart Maritime, which is mainly supported by the Research Council of Norway through the Centres for Research-based Innovation (SFI) funding scheme, project number 237917.

References

Bouman, E.A., Lindstad, E., Rialland, A.I., Strømman, A.H., 2017. State-of-the-art technologies, measures, and potential for reducing GHG emissions from shipping - A review. Transp. Res. D (ISSN: 13619209) 52, 408–421. http://dx.doi.org/10.1016/j.trd.2017.03.022,

Buhaug, Ø., Corbett, J., Endresen, Ø., Eyring, V., Faber, J., Hanayama, S., Lee, D., Lee, D., Lindstad, H., Markowska, A., Mjelde, A., Nelissen, D., Nilsen, J., Pålsson, C., Winebrake, J., Wu, W., Yoshida, K., 2009. Second IMO GHG Study2009. Int. Marit. Organ. (IMO) 240. http://dx.doi.org/10.1163/187529988X00184, http://www.imo.org/blast/blastDataHelper.asp?data{_}id=27795.

Campos, R.M., Soares, C.G., 2016. Comparison and assessment of three wave hindcasts in the north atlantic ocean. J. Oper. Oceanogr. (ISSN: 17558778) 9 (1), 26–44. http://dx.doi.org/10.1080/1755876X.2016.1200249,

Corbett, J.J., Wang, H., Winebrake, J.J., 2009. The effectiveness and costs of speed reductions on emissions from international shipping. Transp. Res. D (ISSN: 13619209) 14 (8), 593–598. http://dx.doi.org/10.1016/j.trd.2009.08.005, http://dx.doi.org/10.1016/j.trd.2009.08.005,

Corbett, J.J., Wang, C., Winebrake, J.J., Green, E., 2007a. Allocation and Forecasting of Global Ship Emissions. Technical Report, Clean Air Task Force, Boston, Massachusetts, USA, p. 26, https://www.researchgate.net/publication/241579973.

Corbett, J.J., Winebrake, J.J., Green, E.H., Kasibhatla, P., Eyring, V., Lauer, A., Winebreak, J.J., Green, E.H., Kasibhatla, P., Eyring, V., Lauer, A., Winebrake, J.J., Green, E.H., Kasibhatla, P., Eyring, V., Lauer, A., 2007b. Mortality from ship emissions: A global assessment. Environ. Sci. Technol. 41 (24), 8512–8518. http://dx.doi.org/10.1021/es071686z,

Di Natale, F., Carotenuto, C., 2015. Particulate matter in marine diesel engines exhausts: Emissions and control strategies. Transp. Res. D (ISSN: 13619209) 40 (600), 166–191. http://dx.doi.org/10.1016/j.trd.2015.08.011,

DNVGL, 2017. Edition august 2017 environmental conditions and environmental loads. Recommended practice DNVGL-RP-C205, August.

ECMWF ERA5, 2018. https://www.ecmwf.int/en/forecasts/datasets/archive-datasets/reanalysis-datasets/era5.

Eyring, V., Isaksen, I.S., Berntsen, T., Collins, W.J., Corbett, J.J., Endresen, O., Grainger, R.G., Moldanova, J., Schlager, H., Stevenson, D.S., 2010. Transport impacts on atmosphere and climate: Shipping. Atmos. Environ. (ISSN: 13522310) 44 (37), 4735–4771. http://dx.doi.org/10.1016/j.atmosenv.2009.04.059, http://linkinghub.elsevier.com/retrieve/pii/S1352231009003653. http://linkinghub.elsevier.com/retrieve/pii/S1352231009003379,

Eyring, V., Köhler, H.W., Van Aardenne, J., Lauer, A., 2005. Emissions from international shipping: 1. The last 50 years. J. Geophys. Res. D: Atmos. (ISSN: 01480227) 110 (17), 171–182. http://dx.doi.org/10.1029/2004JD005619,

Fujibayashi, T., Baba, S., Tanaka, H., 2013. Development of marine SCR system for large two-stroke diesel engines complying with IMO NO x Tier III. in: 27th CIMAC World Congress, Shanghai.

Gregory, D., Confuorto, N., 2012. A practical guide to exhaust gas cleaning systems for the maritime industry, in: EGCSA Handbook, London, UK.

Gully, B.H., Webber, M.E., Seepersad, C.C., Thompson, R.C., 2009. Energy storage analysis to increase large ship fuel efficiency, in: Proceedings of the ASME 3rd International Conference on Energy Sustainability 2009, ES2009, vol. 1. pp. 771–779. ISBN 978-0-7918-4889-0. http://dx.doi.org/10.1115/ES2009-90440, https://www.engineeringvillage.com/blog/document.url?mid=cpx{_}535b58129a8720254M6f7f2061377553{&}database=cpx.

Hepperle, M., 2018. Javafoil. http://www.mh-aerotools.de/airfoils/javafoil.htm.

Hiraoka, N., 2016. Development of low pressure exhaust gas recirculation system for mitsubishi UE, in: 28th CIMAC World Congress, Helsinki. pp. 1–12.

Kampa, M., Castanas, E., 2008. Human health effects of air pollution. Environ. Pollut. (ISSN: 02697491) 151 (2), 362–367. http://dx.doi.org/10.1016/j.envpol.2007.06.012.

Kilic, A., Tzannatos, E., 2014. Ship emissions and their externalities at the container terminal of Piraeus - Greece. Int. J. Environ. Res. (ISSN: 17356865) 8 (4), 1329–1340. http://dx.doi.org/10.1016/j.atmosenv.2009.10.024.

Kim, W.J., Van, S.H., Kim, D.H., 2001. Measurement of flows around modern commercial ship models. Exp. Fluids (ISSN: 07234864) 31 (5), 567–578. http://dx.doi.org/10.1007/s003480100332,

Klimont, Z., Kupiainen, K., Heyes, C., Purohit, P., Cofala, J., Rafaj, P., Borken-Kleefeld, J., Schöpp, W., 2017. Global anthropogenic emissions of particulate matter including black carbon. Atmos. Chem. Phys. (ISSN: 1680-7324) 17 (14), 8681–8723. http://dx.doi.org/10.5194/acp-17-8681-2017, https://www.atmos-chem-phys.net/17/8681/2017/.

Larsen, U., Nguyen, T.V., Knudsen, T., Haglind, F., 2014. System analysis and optimisation of a Kalina split-cycle for waste heat recovery on large marine diesel engines. Energy (ISSN: 03605442) 64, 484–494. http://dx.doi.org/10.1016/j.energy.2013.10.069.

Lindstad, H., Asbjørnslett, B.E., Strømman, A.H., 2011. Reductions in greenhouse gas emissions and cost by shipping at lower speeds. Energy Policy (ISSN: 03014215) 39 (6), 3456–3464. http://dx.doi.org/10.1016/j.enpol.2011.03.044,

Lindstad, E., Bø, T.I., 2018. Potential power setups, fuels and hull designs capable of satisfying future EEDI requirements. Transp. Res. D (ISSN: 13619209) 63 (June 2018), 276–290. http://dx.doi.org/10.1016/j.trd.2018.06.001.

Loukakis, T.A., Sclavounos, P.D., 1978. Some extensions of the classical approach to strip theory of ship motions, including the calculation of mean added forces and moments. J. Ship Res. 22 (1), 1–19, https://trid.trb.org/view/72724.

Lu, R., Turan, O., Boulougouris, E., Banks, C., Incecik, A., 2015. A semi-empirical ship operational performance prediction model for voyage optimization towards energy efficient shipping. Ocean Eng. (ISSN: 00298018) 110 (July 2014), 18–28. http://dx.doi.org/10.1016/j.oceaneng.2015.07.042, http://dx.doi.org/10.1016/j.oceaneng.2015.07.042,

Prpić-Oršić, J., Faltinsen, O.M., 2012. Estimation of ship speed loss and associated CO2emissions in a seaway. Ocean Eng. (ISSN: 00298018) 44, 1–10. http://dx.doi.org/10.1016/j.oceaneng.2012.01.028.

Rakopoulos, C.D., Giakoumis, E., 2006. Review of thermodynamic diesel engine simulations under transient operating conditions. SAE Int. (ISSN: 0148-7191) 2006 (2006–01), 884. http://dx.doi.org/10.4271/2006-01-0884.

Sandvik, E., Nielsen, J.B., Asbjørnslett, B.E., Pedersen, E., Fagerholt, K., 2018. Scenario modelling for operational performance estimation. submitted for publication.

Song, J., wei Gu, C., 2015. Performance analysis of a dual-loop organic rankine cycle (ORC) system with wet steam expansion for engine waste heat recovery. Appl. Energy (ISSN: 03062619) 156, 280–289. http://dx.doi.org/10.1016/j.apenergy.2015.07.019.

Taskar, B., Yum, K.K., Steen, S., Pedersen, E., 2016. The effect of waves on engine-propeller dynamics and propulsion performance of ships. Ocean Eng. (ISSN: 00298018) 122, 262–277. http://dx.doi.org/10.1016/j.oceaneng.2016.06.034.

Tillig, F., Ringsberg, J.W., Mao, W., Ramne, B., 2017. A generic energy systems model for efficient ship design and operation. Proc. Inst. Mech. Eng. Part M: J. Eng. Marit. Environ. (ISSN: 20413084) 231 (2), 649–666. http://dx.doi.org/10.1177/1475090216680672,

Tillig, F., Ringsberg, J.W., Mao, W., Ramne, B., 2018. Analysis of uncertainties in the prediction of ships' fuel consumption–from early design to operation conditions. Ships Offshore Struct. (ISSN: 17445302) 13, 13–24. http://dx.doi.org/10.1080/17445302.2018.1425519.

Yoo, B., Kim, J., 2019. Probabilistic modeling of ship powering performance using full-scale operational data. Appl. Ocean Res. (ISSN: 01411187) 82 (October 2018), 1–9. http://dx.doi.org/10.1016/j.apor.2018.10.013.

Yum, K.K., Taskar, B., Pedersen, E., Steen, S., 2017. Simulation of a two-stroke diesel engine for propulsion in waves. Int. J. Naval Archit. Ocean Eng. (ISSN: 20926790) 9 (4), 351–372. http://dx.doi.org/10.1016/j.ijnaoe.2016.08.004,

Zaccone, R., Ottaviani, E., Figari, M., Altosole, M., 2018. Ship voyage optimization for safe and energy-efficient navigation: A dynamic programming approach. Ocean Eng. (ISSN: 00298018) 153 (October 2017), 215–224. http://dx.doi.org/10.1016/j.oceaneng.2018.01.100.